

# Fractography of Fatigued and Fractured Regions in a Silicon Carbide Whisker Reinforced Alumina Composite

Ashok Kr. Ray, Swapan Kr. Das, Prabir Kr. Roy

National Metallurgical Laboratory, Jamshedpur 831007, Bihar, India

&

S. Banerjee

Research and Development Centre for Iron and Steel—SAIL, Ranchi 834002, Bihar, India

(Received 18 May 1994; revised version received 19 July 1994; accepted 1 August 1994)

## Abstract

*Fatigue cracked and fast fractured regions in four point bend specimens prepared from 25 wt% silicon carbide whisker reinforced alumina composites were examined by Scanning Electron Microscopy. In the fatigue cracked region, the alumina matrix failed mainly in a transgranular mode and the whiskers failed mainly with a flat fracture surface but without pullout. On the other hand, in the fast fractured region, the whiskers failed predominantly by pullout and the alumina matrix failed in a mixed mode with about half in transgranular and the other half in intergranular fracture. Thus, to improve the fracture toughness of the material, the grain boundary strength of alumina and the matrix whisker interfacial bonding should be improved. To increase the resistance to fatigue, the fracture strength of the alumina grains should be improved by using finer  $\alpha$ -alumina particles and the fatigue strength of the whisker has to be increased by improving the uniformity in distribution of  $\beta$ -SiC whiskers during hot pressing.*

## 1 Introduction

Fatigue crack growth rate (FCGR)<sup>1,2</sup> and fracture toughness<sup>1–3</sup> of 25 wt% silicon carbide whisker reinforced alumina ceramic composite have been studied and reported.<sup>1–3</sup> Such studies are important since these materials have potential application in the production of structural components used at elevated temperatures, in high efficiency heat engines and heat recovery systems and for making cutting tools to machine special materials.

When used in such applications, these ceramic components would often encounter monotonic and cyclic loading which produce crack extension. Therefore, the fractographic features of the fatigue failed samples need to be examined to identify the likely micromechanism of crack advance under monotonic and cyclic loading in this composite. Recently, Dauskardt *et al.*<sup>4</sup> have made an extensive fractography of fatigue failed regions in a 15 vol% SiC whisker-reinforced alumina composite. The identification of the fractographic features at the low, medium and high Stress Intensity Range ( $\Delta K$ ) fatigue region as well as in the fast fracture region can give us a clue to the likely mechanisms of fracture in our material.

## 2 Experimental Procedure

The four point bend specimens were sliced, prepared, surface finished and randomised from a 15 mm  $\times$  50 mm  $\times$  12.5 mm preformed billet of 25 wt% silicon carbide whisker reinforced alumina composite material (Fig. 1(a)). The details of fabrication of the billet are given elsewhere.<sup>3</sup>

The alumina powder used was of  $\alpha$ -type.<sup>1</sup> The SiC whiskers had been produced by a carburization process at 1600°C where the sources of silicon and carbon were rice husk ash and rice husk hydrocarbons.<sup>3,5</sup>

The particle size of the alumina powder was less than 1  $\mu$ m. The average whisker diameter was 0.1–0.25  $\mu$ m as revealed in the LT plane of the montage of the ceramic composite investigated here (Fig. 1(b)). The length of the whiskers varied between 10 and 30  $\mu$ m.<sup>3</sup>

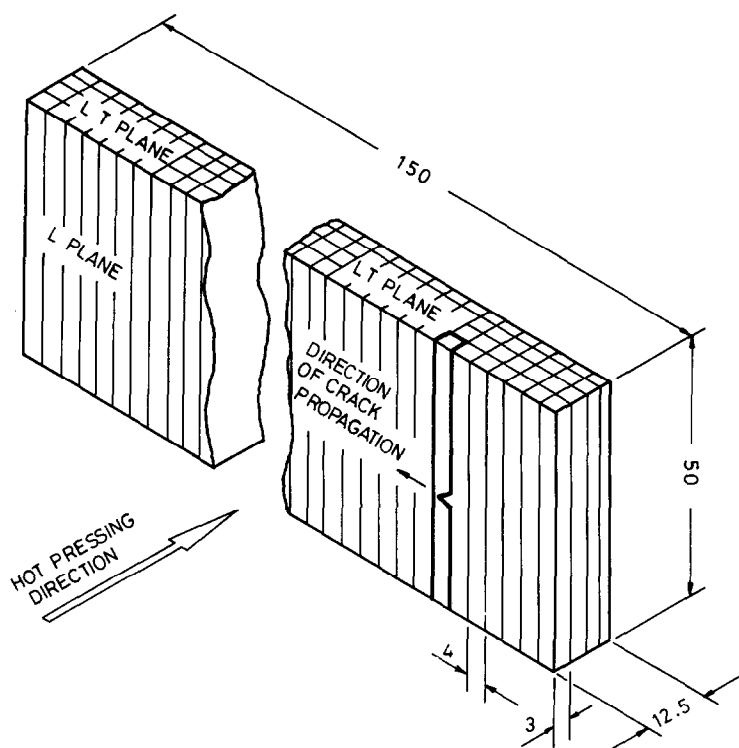


Fig. 1(a). Portion of the billet prepared from the 25 wt% silicon carbide–alumina composite. All dimensions are in mm.

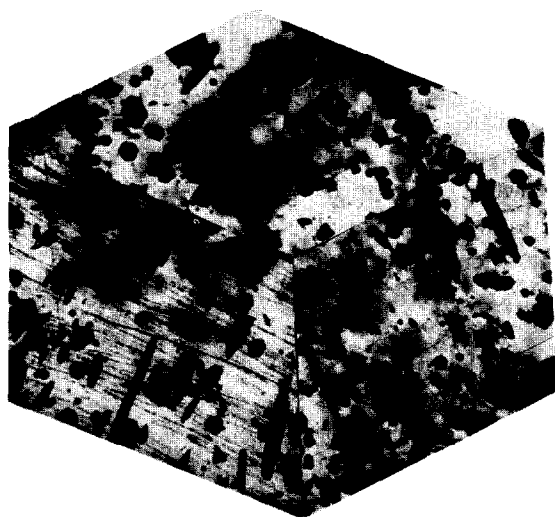


Fig. 1(b). Montage of the microstructures shows distribution of  $\text{SiC}_w$  along the three planes.

The SEM (Scanning Electron Microscope) examination of the fractured surface of the specimens which failed due to premature crack extension during precracking in the conventional bridge fixture,<sup>1,3</sup> showed that the alumina grain size after fabrication varied between 1 and 6  $\mu\text{m}$ . This confirms that during hot pressing, the alumina underwent substantial grain coarsening. In areas where either whiskers were absent or there was evidence of pores (Fig. 2), the grain size was as high as 6  $\mu\text{m}$ . However, in other areas, the majority of the alumina grain size was in the range of 2–4  $\mu\text{m}$ .



Fig. 2. Fracture surface of the composite showing the size and shape of the alumina matrix.

The montage of the ceramic composite revealed the 3D-distribution pattern of the whiskers in the longitudinal (L), long transverse (LT) and short transverse (ST) planes. In the L plane, the whiskers appeared to be randomly oriented as the hot pressing direction is perpendicular to this L plane. During hot pressing, whiskers which are not normal to the L plane get further inclined thus producing the random orientation of the whiskers.<sup>1</sup> Since maximum material flow occurred along the LT planes during hot pressing, the whiskers tend to get oriented parallel to the L plane. In the ST plane, there was a mixture of random orientation as well as normal alignment of the whiskers.

Becher and Wei had concluded in their work<sup>6</sup> that whisker orientation during processing of hot pressed SiC-whisker reinforced alumina leads to anisotropy in both fracture toughness and fracture strength of the composites. In other words, their fracture strengths are limited by the nonuniformity of the distribution of the whiskers, i.e. by the ability to disperse the SiC whiskers. They also found that the dispersion of the whiskers improved by using finer alumina powder and hence an increase in the fracture strength of the composite was observed. Nevertheless, they have clearly observed<sup>6,7</sup> that similar to our composite under investigation (Fig. 1(b)), the whiskers were preferentially aligned perpendicular to the hot pressing axis. This type of distribution of whiskers suggested that a great deal of rearrangement of whiskers and powder occurred in the initial stage of densification of the composites and/or the matrix material underwent considerable deformation or creep during hot pressing.

The dimensions of the billet and the orientation of the four point bend specimens ( $3 \text{ mm} \times 4 \text{ mm} \times 50 \text{ mm}$ ) in the billet is given in Fig. 1(a). The  $4 \text{ mm} \times 50 \text{ mm}$  faces, were normal to the hot-pressing direction so that both the direction of crack propagation (Fig. 3) and the crack plane were parallel to the LT plane (Fig. 1(a)) and normal to the hot-pressing direction.<sup>3</sup> The  $3 \text{ mm} \times 50 \text{ mm}$  faces of the specimen were parallel to the ST plane.

A Vickers indentation produced at 0.8 kN load at the centre of the  $3 \text{ mm} \times 50 \text{ mm}$  face of the sample acted as the crack starter on half of the

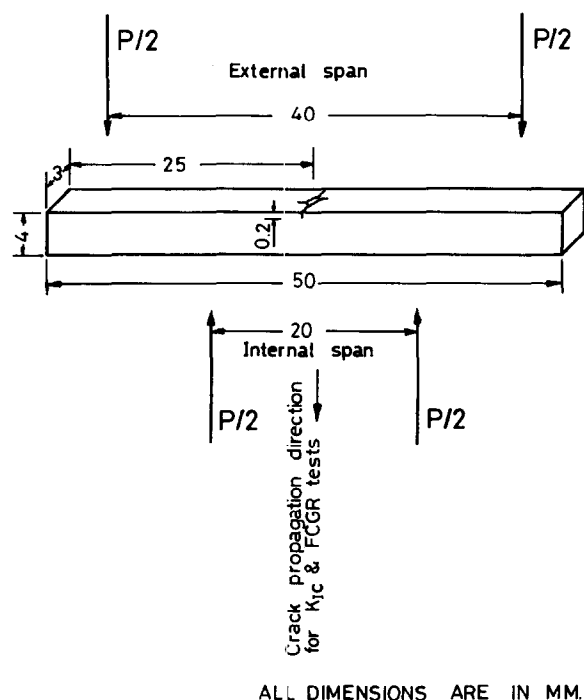


Fig. 3. Indented and precracked specimen for four point bend loading. Cracks are located at the four corners of indentation.

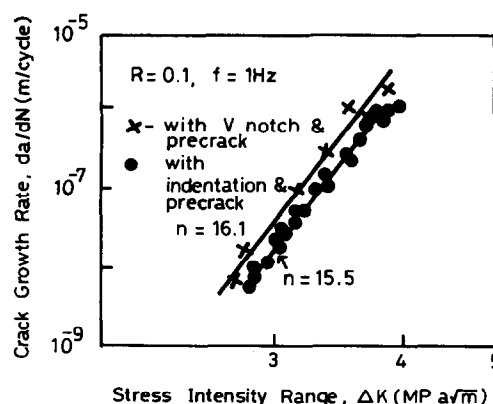


Fig. 4. Fatigue crack growth data of 25 wt% SiC reinforced  $\text{Al}_2\text{O}_3$  composite.

four point bend specimens. On the remaining half, notches were inserted exactly at the centre of the  $3 \text{ mm} \times 50 \text{ mm}$  surface of the specimens with a carborundum wheel to a depth of 0.1 mm. Thereafter, the specimens were subjected to fatigue loading in a servohydraulic test machine MTS-880 (100 kN capacity) to precrack the specimen in an articulated bridge fixture,<sup>2</sup> till the ratio of crack length to width was 0.05 on the ( $4 \text{ mm} \times 50 \text{ mm}$ ) surface of the specimen. Precracking was conducted at a force of 4–5 kN, load ratio,  $R = 0.1$  and frequency,  $f = 20 \text{ Hz}$ . After this, the fatigue crack growth rate in the specimen was determined at increasing values of Stress Intensity Range  $\Delta K$  (Fig. 4), under normal four point bend loading (see Fig. 3) until the ratio of crack length to width was about 0.45–0.5, on the  $4 \text{ mm} \times 50 \text{ mm}$  surface of the specimen. Thereafter, the test to determine the fatigue crack growth rate (FCGR) was terminated and the specimen was subjected to monotonic loading to determine the fracture toughness of the material<sup>1</sup> as per ASTM STP 410.<sup>8</sup> For both FCGR as well as fracture toughness ( $K_{IC}$ ) tests, a 1 kN load range of the MTS-880 test machine was used. The test frequency was 1 Hz and the loading rate was  $0.25 \text{ N s}^{-1}$ . Tests were conducted in laboratory atmosphere and at ambient temperature. The fracture toughness testing produced the fast fracture. The details of fracture toughness and FCGR tests are given elsewhere.<sup>1,2</sup>

The fracture surfaces were coated with a thin film of gold (thickness  $0.02 \mu\text{m}$ ) prior to SEM (Scanning Electron Microscopic examination, in a JEOL JSM 840A microscope).

The three regions, namely low  $\Delta K$  corresponding to  $0.8\text{--}1.8 \text{ MPa}\sqrt{\text{m}}$ ; high  $\Delta K$  corresponding to  $2.8\text{--}3 \text{ MPa}\sqrt{\text{m}}$ ; and, the fast fracture region corresponding to a  $K_{IC}$  value of  $5.9 \text{ MPa}\sqrt{\text{m}}$ , were, at first, identified on the fracture surface at a magnification of 30 X under SEM (Fig. 5) — using the details of the crack growth rate data generated on



Fig. 5. Entire fracture surface. Right-hand side—low  $\Delta K$  region; middle—high  $\Delta K$  region; left-hand side — fast fracture region (FF).

the specimen as a guideline. The difference between the fatigue and fast fracture could, however, be discerned through observation even with the naked eye. The distinction between the low and the high  $\Delta K$  fatigue regions was made from the crack length versus the number of cycles data generated during the fatigue loading of the specimen.

Each region was, at first, carefully scanned at low magnification, to identify the general and uniformly distributed features. Thereafter, it was examined at two different magnifications 4500 X and 7500 X, in order to identify the fractographic features and the mechanism of fracture in the low  $\Delta K$  and the fast fracture regions.

### 3 Fractographic Observations

A summary of the results of the fractographic observations is reported in Table 1.

Table 1 states that, at low  $\Delta K$  (0.8–1.8 MPa  $\sqrt{m}$ ), the whiskers failed predominantly by shearing with a flat or square fracture without any visible evidence of necking; this was typical of fatigue fracture (Fig. 6). However, at high  $\Delta K$  (2.8–3 MPa

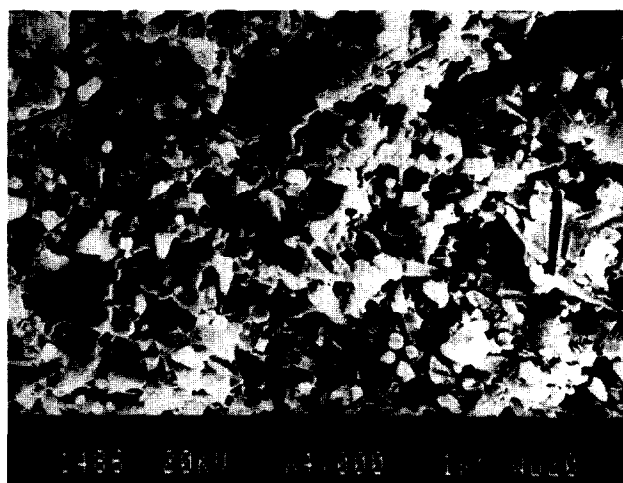


Fig. 6. At low  $\Delta K$  (0.8–1.8 MPa  $\sqrt{m}$ ) region, the majority of the whiskers failed with a square fracture without evidence of large scale pullout.



Fig. 7. At high  $\Delta K$  (2.8–3 MPa  $\sqrt{m}$ ) region the whiskers failed in a mixed mode, i.e. both with a square fracture and also by pullout.

Table 1. Fractographic features in the fatigue and fracture regions in a 25 wt% silicon carbide whisker reinforced alumina

Mechanism of failure		Fatigue		Monotonic
		Low $\Delta K$ 0.8–1.8 MPa $\sqrt{m}$	High $\Delta K$ 2.8–3.0 MPa $\sqrt{m}$	Fracture 5.96 MPa $\sqrt{m}$
Whisker	Pullout (%)	5	40	85
	vs. shear (%)	95	60	15
Matrix	Transgranular (%)	95	55	45
	vs. intergranular (%)	5	45	55
Crack	○ Branching	P	A	A
	○ Deflection	P	A	A
	○ River pattern	P	A	A

P = present; A = absent.

$\sqrt{m}$ ), the whisker failed in two different ways: that is about 60% of the whiskers failed with a flat fracture and the balance failed by pullout (Fig. 7). On the other hand, in the fast fracture region, the whiskers failed predominantly by pullout (Fig. 8).

Table 1 also reports that the matrix alumina grains failed predominantly through transgranular fracture (Fig. 9) at low  $\Delta K$  (0.8–1.8 MPa $\sqrt{m}$ ). In the high  $\Delta K$  (2.8–3 MPa $\sqrt{m}$ ) region, the matrix failed in a mixed mode wherein about 45% of the alumina grains failed by intergranular and the balance by the transgranular mode, as shown in Fig. 10. During monotonic loading, the alumina grains in the fast fracture region also failed in a mixed mode with a slightly increased percentage of intergranular (~55%) and the balance by transgranular mode—as shown in Fig. 11.

It is noteworthy that in the low  $\Delta K$  region, the crack had frequently branched (Fig. 12) and deflected (Fig. 13) while it propagated. River pattern

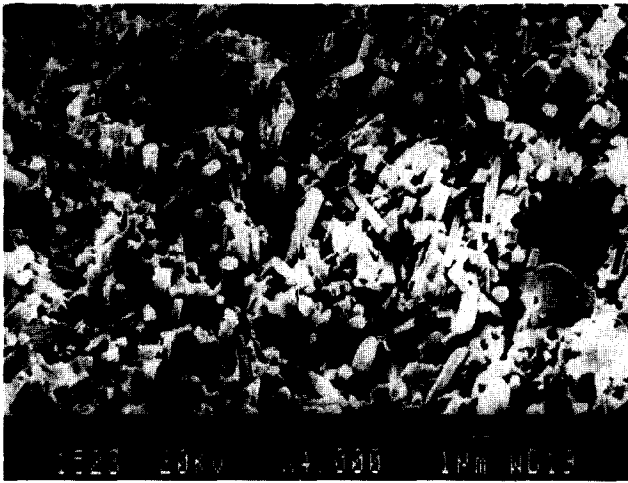


Fig. 8. In the fast fracture region ( $K_{IC} = 5.9 \text{ MPa}\sqrt{\text{m}}$ ), whiskers failed predominantly by pullout mechanism.



Fig. 9. At low  $\Delta K$  region, the alumina matrix failed predominantly through transgranular fracture.



Fig. 10. At high  $\Delta K$  region, the alumina grains failed in a mixed mode, i.e. intergranular (~45%) and transgranular (~55%).

markings with steps (Fig.14) were also present in the cleavage facets. However, in the fast fracture region, the branching and deflection of the crack were virtually absent.

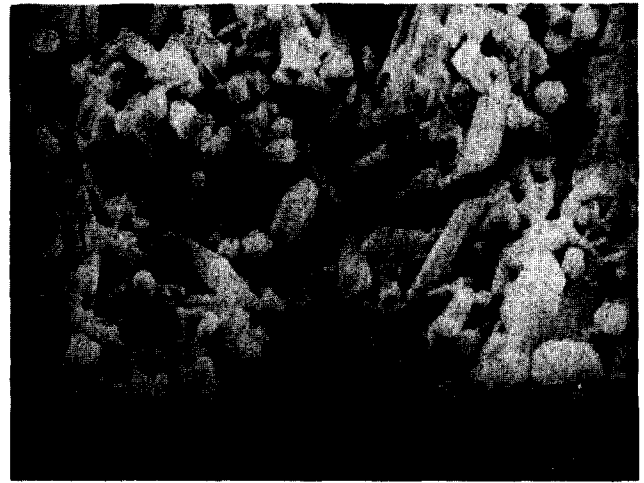


Fig. 11. In the fast fracture region (monotonic loading), the alumina grains failed in a mixed mode, i.e. intergranular (~55%) and transgranular (~45%).



Fig. 12. Crack branching in the low  $\Delta K$  region.

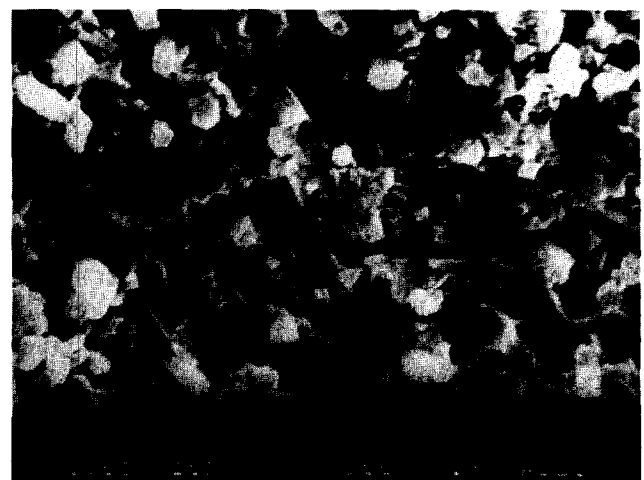


Fig. 13. Crack deflection in the low  $\Delta K$  region.

#### 4 Discussion

Twenty-five weight percent silicon carbide whisker reinforced alumina composite is susceptible to a fatigue crack growth phenomenon<sup>1,2</sup> (Fig. 4), which is similar to that in the case of metallic

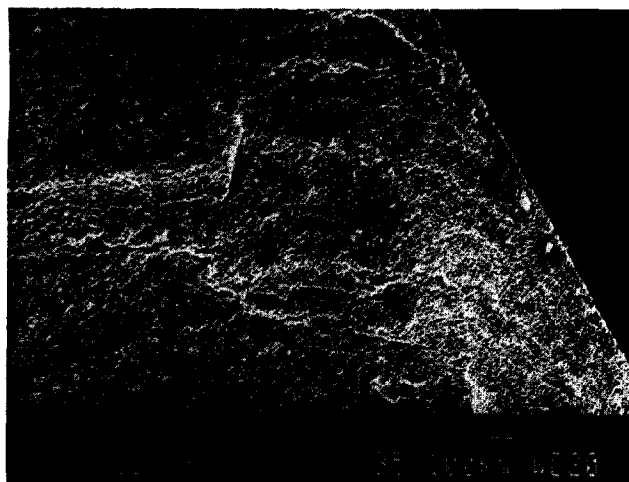


Fig. 14. River pattern marking with steps in the low  $\Delta K$  region (YZ—modulation SEM image).

metals, but with a higher crack growth exponent ( $n = 15.5$ ). Figure 4 shows that the FCGR data of this material fits the usual Paris equation  $da/dN = A(\Delta K)^n$ .

Since the manner of failure of the whiskers and the  $\alpha$ -alumina grains were entirely different in the low  $\Delta K$  fatigue and the fast fracture regions, the schemes of crack growth under these two conditions are discussed separately, to focus on their contradistinctions.

#### 4.1 Low $\Delta K$ fatigue region

During fatigue loading at the low  $\Delta K$  regions, where  $\Delta K = 0.8\text{--}1.8 \text{ MPa } \sqrt{\text{m}}$  the alumina grains of the matrix failed mainly by transgranular cleavage with frequent crack branching and crack deflection. Also, the cleavage facets revealed river pattern and steps. At low  $\Delta K$ , the  $K_c$  values and consequently the traction force ahead of the crack tip, were not adequate to promote intergranular fracture.

At low  $\Delta K$ , the amount of crack extension is very low. So even though the energy dissipated per cycle is low, the number of cycles and the cumulative energy required for a given amount of crack extension is quite significant and can thus account for the higher surface area required for the various features encountered like crack branching, river pattern and steps.

At low  $\Delta K$  fatigue, the whisker could fail in three different modes

- pullout,
- tensile fracture,
- fatigue.

Table 1 shows that only a few of the whiskers failed due to pullout at low  $\Delta K$  fatigue. This naturally indicated that the maximum traction forces generated ahead of the crack tip during the low  $\Delta K$  fatigue was not adequate to produce a pullout.

Thus, it is likely that the whiskers continue to bridge the crack even after some of the surrounding alumina grains had failed by transgranular cleavage. Therefore, under these circumstances, the whisker could fail due to tensile fracture or fatigue.

One might rule out the possibility of tensile fracture if one had examined the relative values of strength and Young's modulus reported in Refs 9 and 10. The fracture strength of the whisker is about 6.5–7 times higher than that of alumina. Accordingly, the tensile fracture of the whisker was unlikely if the traction forces ahead of the crack tip were to be distributed in proportion to the relative cross sections of the whisker and alumina in the plane of the crack. Even if the whiskers were to carry the major part of the traction forces ahead of the crack tip, the high traction forces would produce failure by pullout rather than by tensile fracture, as was observed in the fast fracture region where  $K_{IC}$  values and consequently the traction forces, were high.

Since the possibility of large scale failure by pullout or tensile fracture was discounted, whiskers were most likely to fail by fatigue. At low  $\Delta K$ , the whiskers which had bridged the crack after the surrounding alumina grains had failed by cleavage, would continue to experience fatigue loading, then failed with a square fracture which is typical of fatigue. The fatigue failure of the silicon carbide whisker under such circumstances, could be significantly influenced by the stacking fault such as is reported Ref. 11 in Fig. 15, since such fault could be responsible for nucleating the fatigue crack. However, this aspect needs careful study.

Since the cleavage of the  $\alpha$ -alumina grains probably occurred before the whiskers (located mainly at the grain boundaries) had failed, it was necessary to improve the fatigue resistance of the  $\alpha$ -alumina grains. This apart, the dislocation pile-up



Fig. 15. TEM of  $\beta$ -SiC whisker showing stacking fault by dark field and bright field techniques.

model<sup>12</sup> would obviously indicate that the cleavage failure of  $\alpha$ -alumina could be prevented through the refinement of alumina grains in the aggregate structure. The size of alumina grains varied between 1 and 6  $\mu\text{m}$ . In this context, one should note that one could obtain higher resistance to low  $\Delta K$  fatigue, if ultra-fine or nano-size alumina grains, such as that produced by the solgel technique, were to be used to fabricate this composite.

A schematic view of crack propagation mechanism is represented in Fig. 16(a). It illustrates that at low  $\Delta K$  fatigue, the matrix failed predomi-

nantly by transgranular cleavage and the advancing crack frequently branched and tilted and twisted in its course of deflection. Since the whiskers were predominantly located at the grain boundaries and the crack propagation along the grain boundary at low  $\Delta K$  fatigue was negligible, the possibility that the crack would encounter these whiskers as it advances would be rather low. Only a few of those whiskers which had bridged the crack with an orientation normal to the advancing crack plane, could fail by pullout. The other whiskers were likely to fail by directly experiencing fatigue loading. This could explain why

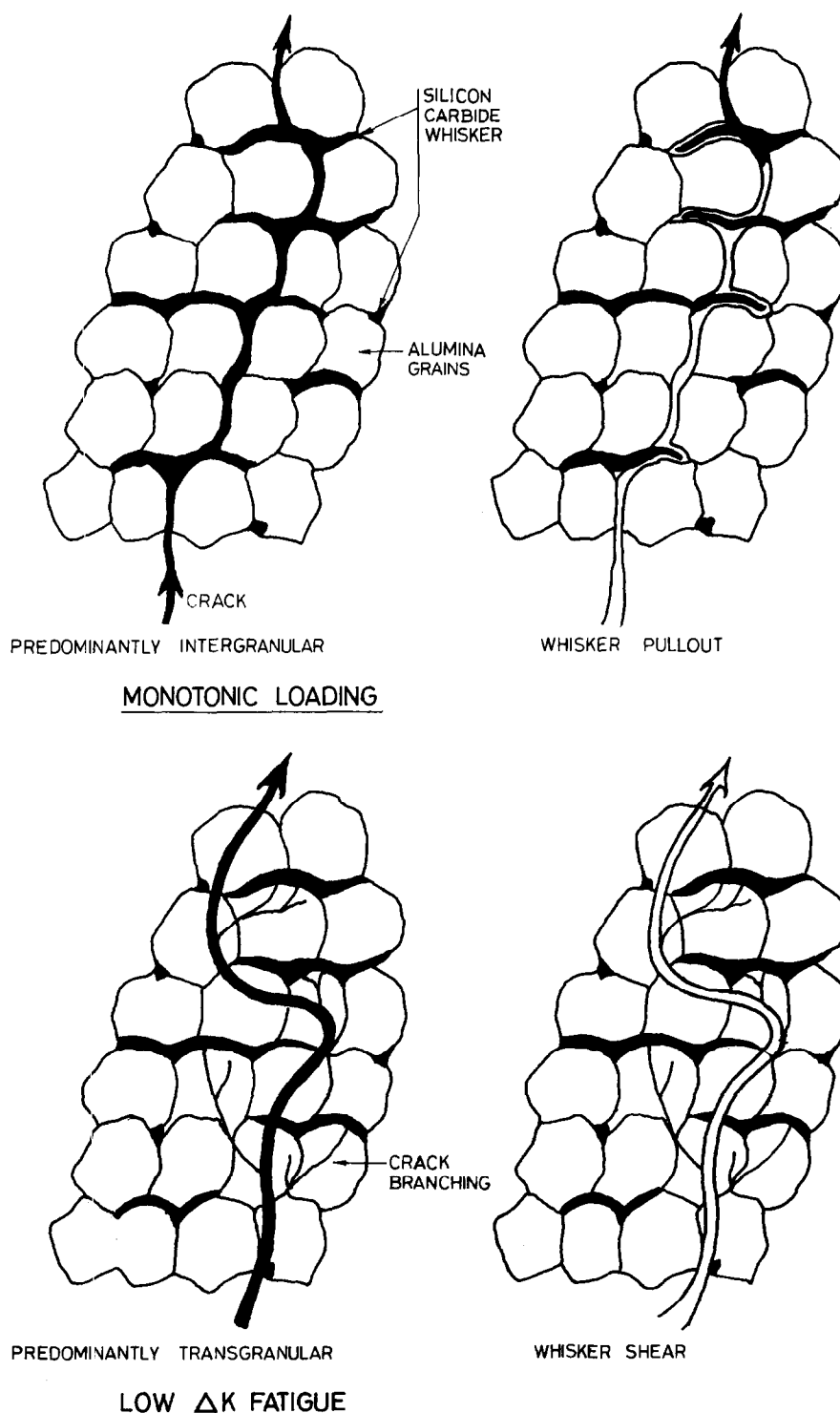


Fig. 16. Schematic of the crack propagation during monotonic and cyclic loading.

at low  $\Delta K$  fatigue, the majority of the whiskers failed with a square fracture and without pullout.

#### 4.2 Fast fracture region

During the fast fracture under monotonic loading such as during the fracture toughness testing, some of the  $\alpha$ -alumina grains of the matrix failed by intergranular fracture; the others failed by transgranular cleavage. The value of  $K_{IC}$  during such monotonic loading was 5.9 MPa  $\sqrt{m}$ . At such values of  $K_C$ , the traction force generated ahead of the crack tip was adequate to produce the intergranular failure in those grains which were favourably oriented with respect to the direction of the traction force. Debonding and pullout of those whiskers at the fractured grain boundaries would therefore occur.

It is difficult to summarise from the fractographic features as to which of these, i.e. transgranular cleavage or intergranular fracture, occurred, at first, under monotonic loading.

After some of the grains had failed through the intergranular mode, the other neighbouring grains which were less favourably oriented or which were strongly anchored by the whiskers across the grain boundaries, failed through transgranular cleavage.

The pullout of the whiskers could be avoided if the whisker  $\alpha$ -alumina interfacial strength was improved or if finer and more numerous whiskers and also finer  $\alpha$ -alumina particles were used in fabricating the composite. Similarly, the intergranular fracture could be avoided by strengthening the boundaries.

As illustrated schematically in Fig. 16(b), the fracture due to monotonic loading showed a substantial amount of intergranular failure of the matrix and pullout of the whiskers. Crack deflection, branching and the characteristic river pattern marking with steps, were absent in this region.

The matrix failure was predominantly intergranular. Nevertheless, the whiskers were located mainly at the grain boundaries. Therefore, the probability of the advancing crack front interacting with the whiskers was extremely high. The whiskers tending to bridge the advancing crack quite frequently would therefore get debonded and pulled out—which is schematically illustrated and shown in Fig. 16(b). This justifies the fact that during the monotonic fracture, failure of whiskers by the pullout mechanism was frequently observed in the fractograph.

During fatigue loading at high  $\Delta K$ , mechanism of fracture was an intermediate situation between the two extreme cases: that is between the case of monotonic fast fracture and that of the low  $\Delta K$  fatigue fracture.

Since the ceramic material is often expected to survive both monotonic and fatigue loading, one could make the following general observations based on the scheme of crack growth under the two conditions as discussed above.

To prevent fracture failure of this ceramic material under monotonic loading, its microstructural features would have to be strengthened to avoid intergranular fracture of  $\alpha$ -alumina and the pullout of the whisker. This requires that the grain boundary strength of  $\alpha$ -alumina and the whisker—matrix interfacial strength should be increased. Similarly, to retard crack extension during low  $\Delta K$  fatigue, intergranular cleavage fracture of  $\alpha$ -alumina grains and fatigue failure resistance of the silicon carbide whiskers should be improved, possibly by using finer  $\alpha$ -alumina powder<sup>6,7</sup> and by improving the uniformity of distribution of whiskers in the matrix during hot pressing.<sup>6,7</sup>

#### 5 Conclusions

The micromechanism of fracture of a 25 wt% silicon carbide whisker reinforced alumina composite when loaded in fatigue was quite different from that when loaded monotonically. Consequently, the fractographic features in the two instances of loading were significantly different.

When loaded in fatigue, the alumina matrix failed in a transgranular mode and the whiskers failed by producing a flat fracture but without their pullout.

When loaded monotonically, the whiskers predominantly failed by pullout and the alumina matrix failed in a mixed mode with about 55% in intergranular and the balance in transgranular mode. Whereas the grain boundary strength of  $\alpha$ -alumina and the whisker—matrix interfacial bonding should be increased to produce increased resistance to failure under monotonic loading. The fatigue failure resistance of the composite could be improved by improving the cleavage strength of the  $\alpha$ -alumina grains, i.e. by using finer  $\alpha$ -alumina particles and by increasing the fatigue strength of the whiskers by improving the uniformity in the distribution of  $\beta$ -SiC whiskers during hot pressing.

#### Acknowledgements

The authors gratefully acknowledge the help and advice of Mr N. K. Das and Professor O. N. Mohanty in the SEM work. The authors are thankful to Professor P. Ramachandrarao Director-National Metallurgical Laboratory, for allowing us



to publish this work and to NIST (National Institute of Standards and Technology) NBS-USA for supplying us the ceramic specimens.

## References

1. Ray, A. K., Fuller, E. R. & Banerjee, S., Fatigue crack growth rate and fracture toughness of 25 weight percent silicon carbide whisker reinforced alumina composite with residual porosity. Submitted to *J. Eur. Ceram. Soc.* (1994).
2. Ray, A. K. & Banerjee, S., Precracking of ceramic specimen and determination of fracture crack growth rate of 25 wt% SiC reinforced  $\text{Al}_2\text{O}_3$  composite. Accepted for publication in *J. Am. Ceram. Soc.* (1995).
3. Krause, R. F. Jr & Fuller, E. R. Jr, Fracture resistance behaviour of silicon carbide whisker-reinforced alumina composites with different porosities. *J. Am. Ceram. Soc.*, **73**(3) (1990) 559–66.
4. Dauskardt, R. H., James, M. R., Porter, J. R. & Ritchie, R. O., Cyclic fatigue crack growth in a SiC whisker—reinforced alumina ceramic composite. *J. Am. Ceram. Soc.*, **75**(5) (1992) 759–71.
5. Cook, J. L. & Rhodes, J. R., Silicon carbide whiskers. Presented at the 88th *Annual Meeting of the American Ceramic Society*, Chicago, IL, April 28, 1986 (Engineering Ceramics Division, Paper No. 18-C-86).
6. Becher, P. F. & Wei, G. C., Toughening behaviour in SiC-whisker-reinforced alumina. *J. Am. Ceram. Soc.*, **67**(12) (1984) 267–9.
7. Wei, G. C. & Becher, P. F., Development of SiC—whisker—reinforced ceramics. *J. Am. Ceram. Soc.-Bull.*, **64**(2) (1985) 298–304.
8. Brown, W. F., Jr & Srawley, J. E., *American Society for Testing and Materials STP—410*. ASTM, Philadelphia, PA, 1966.
9. Ray, A. K., Mohanty, G. & Ghose, A., Effects of catalysts and temperature on silicon carbide whiskers formation from rice husk. *J. Mater. Sci. Lett.*, **10** (1991) 227–9.
10. Fisher, E. S., Manghnani, M. H. & Routbort, J. L., Study of the elastic properties of  $\text{Al}_2\text{O}_3$  and  $\text{Si}_3\text{N}_4$  material composites with SiC, whisker reinforcement. *High Performance Composites for the 1990s*, ed. S. K. Das, C. P. Ballard and F. Marikar, The Minerals, Metals and Materials Society, 1991.
11. *Reinforcing Tomorrows Technology*. Ceram. Indust. April (1992).
12. Kingery, W. D., Bowen, H. K. & Uhlmann, D. R., *Introduction to Ceramics*, 2nd ed., John Wiley and Sons, Inc. New York, 1976, p. 795.